Nucl. Sci. and Tech., Vol.10, No. 2 (2020), pp. 15-25

Nuclear Science and Technology

Journal homepage: https://jnst.vn/index.php/nst

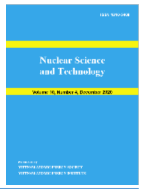

Numerical Investigation of Fluid – Structure Interaction (FSI) on Sodium Leakage Accident at Prototype Fast Breeder Reactor Monju

Hoang Tan Hung, Bui Thi Hoa, Hoang Minh Giang

Institute for Nuclear Science and Technology, 179 Hoang Quoc Viet, Nghia Do, Cau Giay, Ha Noi
Email: hoangtanhung1991@gmail.com

Abstract: This study presents a numerical investigation of fluid-structure interaction about sodium leakage accident at prototype fast breeder reactor Monju. The dynamic forces of sodium liquid flow acting on the thermowell are the main cause of fatigue failure, which leads to the occurrence of thermowell cracking due to intense stresses and high fatigue-cycle. Since the location and magnitude of these stresses are unknown, an analysis of the vibrational characteristics and stresses caused by FSI was performed by using ANSYS to prevent similar accidents in the future. The most dangerous case was found for FSI analysis by comparisons between the natural frequency of thermowell and vortex shedding frequency at several operating conditions. The results showed that a stress concentration location is similar to the location of broken thermowell, and the amplitude of stress is large enough for fatigue damage.

Keywords: *Monju, Sodium leakage accident, FSI, ANSYS.*

I. INTRODUCTION

Monju is a fast breeder reactor (FBR) that has been developed in Japan for a long – term research, development, and utilization program in nuclear energy. On 8th December 1995, the reactor suffered a serious accident with sodium leaked through a temperature sensor due to a break of thermowell inside a secondary pipe resulting from intense vibration. A study on sodium leakage at Monju was performed in [1] to investigate the causes and consequences of the accident. From the results, it was concluded that the breakage of the thermowell was caused by high cycle fatigue of the well tube tip due to Vortex-Induced Vibration (VIV) phenomenon.

In the study of Ref. [2], it was found that vortex-induced vibration depends on the specific range of reduced velocity. Therefore, a range of the reduced velocity was created using the experimental facility to avoid that phenomenon. The purpose of this experiment was to study the interaction between water and circular cylinder structure under the operational conditions of the Monju reactor.

On the other hand, to prevent the sodium leakage accident, the improvement of thermowell design was obtained by means of an analytical study using the finite element method (FEM) [3]. Various designs of thermowell were taken into account. The results showed that the design of thermowell with a continuous low-gradient slope and no neck could avoid the effects of VIV.

It can be seen that, after the sodium leakage accident at the Monju reactor, many

https://doi.org/10.53747/jnst.v10i2.33
Received 28 February 2020, accepted 21 April 2020

studies were performed to find the cause of the accident and also to prevent the accident from happening again. This prevention could be done by the thermowell design and its working condition improvement. However, the number of studies on thermowell stress concentration prediction under the operational condition still limited. Therefore, it is necessary to perform a study on the prediction of the stress concentration of thermowell. On the other hand, the Monju accident happened due to the VIV phenomenon as a consequence of FSI. One study on the consequence of FSI using ANSYS has done [4] to predict thermowell stress concentration on the steam temperature sensor. Base on this paper, our work focus on ANSYS simulation to predict the stress concentration of Monju's thermowell.

In this study, following the study as mentioned in [4], an analysis of FSI between sodium liquid and Monju's thermowell will be performed by using ANSYS. Two approaches of one-way FSI and two-way FSI are applied to investigate the VIV phenomenon to find the stress concentration location and the stress amplitude acting on Monju's thermowell.

II. EXPERIMENTAL FACILITY AND CALCULATING METHODS

A. Overview of Monju facility

The Monju fast-breeder reactor is a sodium-cooled reactor operating at a thermal output of 714 MW and has an electrical generating capacity of 280 MW. Liquid sodium is used in the primary and secondary cooling systems. An accident occurred due to the failure of a thermowell located in the secondary cooling system in the course of power buildup test programs. The thermowell was broken apart by high cycle fatigue failure. Figure 1 shows the configuration of thermowell before and after the accident. The tip of the well-tube was lost and the thermocouple was bent approximately 45 degrees from the original position. Thermowell is a type of step-shank with its whole length of 185.5 mm and its thickness of 3 mm as shown in Figure 1. It is made of 304 stainless steel, which is 8000 kg/m^3 in density, Young modulus, E, is in the range of 193 – 200 GPa, and the Poisson ratio equal to 0.29 [5].

From the operation history of the secondary loop of the Monju fast breeder reactor [6] and thermodynamic and transport properties of sodium liquid [7], the characteristics of sodium liquid flow depend on the history of the secondary heat transport system operation is presented in Table I.

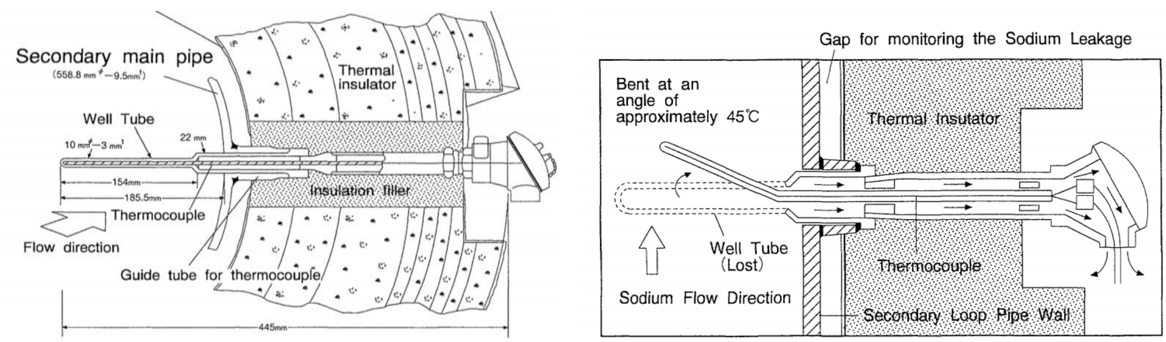

Fig. 1. Thermowell configuration before and after the accident [8]

Table I. Characteristics of sodium liquid flow in the secondary heat transport system

	Temperature (℃)	Velocity (m/s)	Dynamic viscosity (10^{-4} Pa.s)	Density (kg/m^3)	Reynold number
Case 1	200	5.20	4.52	903.0352	1.04×10^5
Case 2	200	2.08	4.52	903.0352	4.15×10^4
Case 3	450	2.08	2.55	846.2525	6.92×10^4
Case 4	485	2.08	2.41	838.1427	7.23×10^4

B. Calculation Method

The VIV phenomenon is the main cause of damaging the thermowell of the Monju reactor. Vortices were formed and detached periodically from either side of cylindrical bodies causes an unsteady oscillating flow. An asymmetrical flow pattern develops around the body because of the periodic shedding and changes in the pressure distribution behind the body. Vortex shedding occurs at a certain frequency, which is called vortex shedding frequency (f_S). This frequency depends on flow velocity U and the cylinder diameter D, Strouhal number (St) and formulated as [9]:

$$St = \frac{f_S D}{U} \tag{1}$$

As a result of the periodic change of the vortex shedding, the pressure distribution on the cylinder outer surface may also change periodically, thereby generating a periodic force on the cylinder surface. Each cylindrical body has its natural frequencies (f_N). If the vortex shedding frequency (f_S) is close to one of the natural frequencies (f_N), resonance could have happened. Then, as a result, the cylindrical bodies start to vibrate with the same frequency as the vortex shedding frequency, called the lock-in phenomenon. This lock-in phenomenon could lead to large amplitude vibrations of structure, which in turn causes fatigue damage. However, this situation occurs in a range of frequencies, not a single value of frequency as the normal resonance. The following condition is given to avoid fatigue damage [10]:

$$f_S < 0.4\, f_N \tag{2}$$

Because the Monju reactor was operated under several conditions, it is necessary to find the most dangerous case to perform FSI analysis by using the criteria of equation (2). Firstly, Modal analysis was applied to determine the natural frequency (f_N) and the mode shape of the structure. Secondly, 2D flow analysis in Fluent was conducted to determine the vortex shedding frequency of different flow conditions. A comparison between the natural frequency of structure (f_N) and vortex shedding frequency (f_S) could show the most dangerous case to perform FSI analysis. Finally, the FSI calculation was performed to analyze the location and value of stress concentration on the thermowell tube. The value of stress concentration was compared with the endurance limit of material (S_E). The diagram of the analysis process is shown in Figure 2.

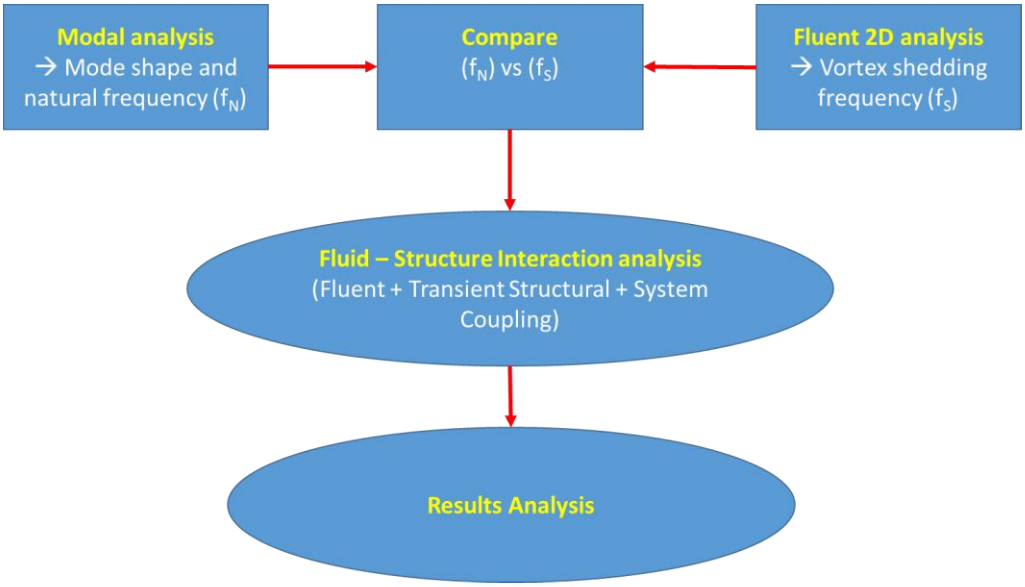

Fig. 2. Analysis process

1. Modal analysis

The vibrational characteristics of the structure were determined using Modal analysis. These characteristics which contain natural frequencies and mode shapes of the structure are important in designing a structure subjected to a dynamic load. The basic equation used in the Modal analysis for free, undamped vibration which is given [11] as followings:

$$([K]) - f_i^2[M]\{\phi_i\} = \{0\} \quad (3)$$

Where $[\boldsymbol{K}]$ and $[\boldsymbol{M}]$ are the stiffness and mass matrix; $\boldsymbol{\phi_i}$ is a mode shape vector (Eigenvector) of mode i and $\boldsymbol{f_i}$ is a natural frequency of mode i.

Dynamic response of structures could occur under the harmonically varying load, whose frequencies are used to determine whether the resonance occurs or not. If the frequency of vortex shedding (fs) is close to one of the natural frequencies (f_i) of structures, it may lead to the resonance which causes the failure of the structure. Therefore, it is an essential process to find out the natural frequencies and mode shapes of a structure to find the most dangerous case of flow operation of the Monju reactor.

2. 2D Fluent analysis

The 2D Fluent analysis was performed with a typical cross-section of thermowell. 2D model of thermowell and mesh is showed in Figure 3. As it can be seen in Table I, all of the cases have Reynold numbers greater than 10^4, so the standard k - ω (k is the turbulence kinetic energy (m^2/s^2) and ω is the specific rate of dissipation (m^2/s^3)) turbulence model for near-wall interactions model was chosen for simulation. By using a Fast Fourier Transformation (FFT) of velocity, the vortex shedding frequency of different flow conditions was found and compared with natural frequencies from Modal analysis.

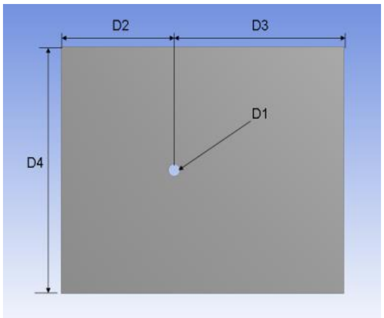

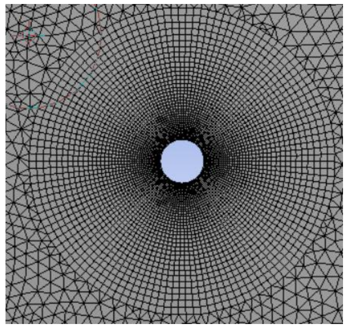

D1 = 0.01 m = D   D2 = 0.14 m = 14 D   D3 = 0.16 m = 16 D   D4 = 0.15 m = 15 D

Fig. 3. Model of 2D Fluent analysis at the typical cross-section of thermowell

3. FSI analysis

From the previous results, the most dangerous case was selected for FSI analysis. An interface surface between the solid and the fluid domain always existed in FSI analysis. At this interface, both the governing equations and the boundary conditions from the fluid and solid domain should be continuous. A set of coupling boundary conditions, therefore, is introduced. The interface conditions of displacement continuity, Eq. 4, and traction equilibrium (momentum transfer), Eq. 5 must be satisfied along the fluid-structure boundary [9].

$$d_f = d_s \tag{4}$$

$$P_f = P_s \tag{5}$$

Where d_f and d_s are the deformations of fluid and structure domain; P_f and P_s are the pressure of the fluid and structure domain.

The analysis in this study was divided into two simulations, one-way FSI and two-way FSI, to compare the structural response to static and dynamic load.

In the one-way FSI simulation, the focus is on the effect of sodium flow to the thermowell, so the pressure load data only transferred from Fluent solver to the Structure solver as mentioned in equation 5. However, the solid displacement is not transferred back to the Fluent solver. Therefore, pressure data taken from the Fluent solver is imported to the Structure solver.

The one-way FSI simulation is one-way data transport. Nevertheless, the two-way FSI simulation is more complicated because of their interaction between both solvers. The motion of thermowell simulation is solved in the Transient structure, while the motion of flow is solved in Fluent. The System Coupling controls the solution process as well as data transfers between the two analysis systems. Force data from the motion of flow is received by the Transient structure as mentioned in equation 5. After finishing the Structural solving process, the displacement data from the motion of thermowell is received by the Fluent as mentioned in equation 4 then the Fluent solves the fluid behavior over time. As a consequence, the mesh is deformed according to the response of the structure. Displacement values are interpolated to the fluid mesh which results in deformation of the fluid domain.

In summary, the one-way FSI approach uses only the traction equilibrium, Eq. 5, and the data is transferred from Fluent solver to the Structure solver. In contrast, the two-way FSI approach uses both the traction equilibrium, Eq. 5, and the displacement continuity condition, Eq. 4.

Through the two-way FSI process using both Eq. 4 and 5, displacement values are updated to the fluid mesh.

C. Verification of the Modal and FSI calculation models

To demonstrate further the validity of the Modal and FSI calculation models with oscillation problems, the oscillation of an exemplary vertical plate in a cavity filled with fluid was investigated. Figure 4 shows a schematic diagram of the oscillation problem [12].

A thin plate is anchored to the bottom of a closed cavity filled with fluid. There is no friction between the plate and the side of the cavity. During the first 0.5 seconds, a uniformly distributed load of 30 N/m is applied to distort it. Once this load is released, the plate oscillates back and forth to regain its equilibrium, and the surrounding air damps this oscillation. The flexible plate has Young's modulus of E = 2.5 MPa, a Poisson's ratio of ν = 0.35, and a density of 2550 kg/m^3. The simulation with fluid density is ρ_F = 1kg/m^3, and three different dynamic viscosities of the fluid μ = 0.2, 1.0, and 5.0 Pa.s are considered for the flow conditions.

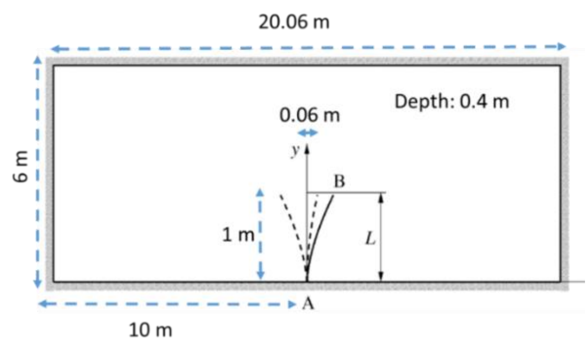

Fig. 4. Geometry of oscillating plate (not drawn to scale)

In Modal analysis, a fixed support constraint is needed to hold the bottom of the thin plate in place and the set up to find the first natural frequency and mode shape of the plate. The result of Modal analysis showed that the value of the first natural frequency of the plate is 0.317Hz.

An interface between the solid domain and the fluid domain was created for data transferring, as mentioned in the previous section of FSI analysis. Displacement values of the plate are interpolated to the fluid mesh using two-way FSI. Figure 5 (a, b, c) shows the horizontal displacement of the free end of the plate comparisons between our calculation results with that of Glück [12] at three different viscosities of fluid. Our results have the same tendency as Glück: the higher the viscosity of the fluid, the faster the plate is damped and reaches the equilibrium state. However, there exist slight discrepancies in the frequency and the amplitude of oscillation. A different mesh model could be the leading cause of these discrepancies. Sodium liquid is the fluid domain with specific viscosity and density in FSI analysis of Monju's thermowell. If its density and viscosity change, its behavior could be different. In four different cases listing in Table I, lower viscosity of sodium liquid in the range of 2.41 – 4.52×10^{-4} Pa.s causes a lower damping coefficient; it may take a longer time for the plate to reach the equilibrium state.

From the analytical calculation, the first natural frequency of the simplified of a clamped beam is defined as follows [12]:

$$f_1 = 0.5595 \frac{1}{L^2} \sqrt{\frac{EI}{m/L'}} \tag{6}$$

Where I is the polar moment of inertia and m is the total mass.

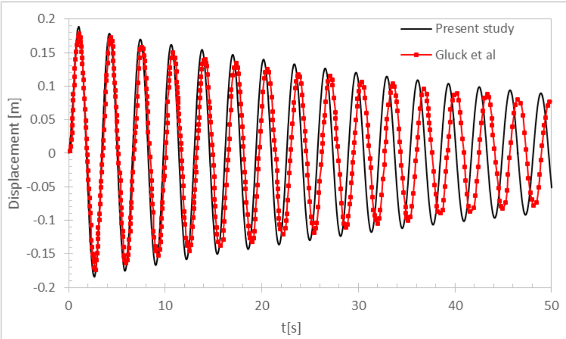

(a) μ = 0.2 Pa.s

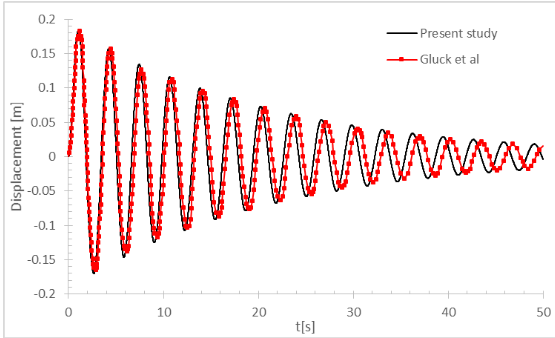

(b) μ = 1.0 Pa.s

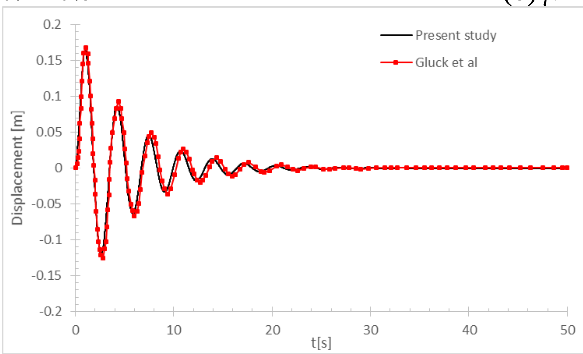

(c) μ = 5.0 Pa.s

Fig. 5. Comparison of the displacements of the free end of the beam form three different fluid viscosities with Glück et al (2001) [12]

However, our result only showed the displacement of the plate in time. Therefore, FFT is used to find the frequency of the plate to compare it with the analytical calculations. Applying the FFT of the displacements to the case of the dynamic viscosity of 0.2 Pa.s, the first natural frequency of the plate can be found, f= 0.319 Hz. The analytical value of f_1 = 0.300 Hz is approximately equal to the simulation value of Modal analysis 0.317 Hz (5.6% difference) and FSI analysis 0.319 Hz (6.3 % difference). It can be seen that the characteristic of the oscillation of the plate is nearly the same with the thermowell on the Monju reactor. Therefore, the Modal and FSI calculation models can be applied for fundamental analysis of the oscillation of thermowell.

III. RESULTS AND DISCUSSION

Because the lock-in can occur when the frequency of vortex shedding (fs) is close to one of the natural frequencies (f_i) of structures, the Modal simulation set up to find the first six natural frequencies of thermowell. Table II shows the results of Modal analysis, the value of frequencies are nearly equal in pair because of the symmetry characteristic of the geometry model of y and z-direction.

Table II. Natural frequency of thermowell

Mode	1	2	3	4	5	6
Natural frequency f_N (Hz)	261.15	261.22	1611.70	1612.00	4327.20	4327.50

Four cases of 2D Fluent analysis were performed to find the frequency of vortex shedding (fs) of each flow condition with a typical cross-section of thermowell. The velocity of sodium flow is 5.20 m/s and 2.08 m/s, corresponding to the 100% and 40% flow operation. Figure 6 shows that the vortex shedding appears behind the thermowell, and the change of drag and lift forces coefficient is periodical in Case 1. The frequency of vortex shedding (fs) of each case is found by using FFT. A detailed comparison between the average natural frequency of structure (f_N) and vortex frequency fo fluid (f_S) for Mode 1 and Mode 2 is shown in Table III. From Eq. 2, it can be seen that the safe cases could be reached if the frequency ratio, f, is smaller than 0.40, and it could be dangerous in reverse situations. Except for Mode 1 and 2, it can be seen that f is much smaller than 0.40 in other modes with higher frequencies. The most dangerous case could occur in Mode 1 and 2. Therefore, higher natural frequency comparisons are not necessary. The results show that the most dangerous case of flow condition can lead to fatigue damage is Case 1 with ratio $f = f_S / f_N = 0.65$. The obtained result in Case 1 was in good agreement with that in [1].

Table III. Comparison of natural frequency of thermowell and vortex shedding frequency

	Vortex shedding frequency f_S (Hz)	**Average natural frequency f_N (Mode 1 and mode 2) (Hz)**	**Ratio $f = f_S/ f_N$**
Case 1	170.94	261.185	**0.65**
Case 2	64.10	261.185	0.25
Case 3	64.10	261.185	0.25
Case 4	64.10	261.185	0.25

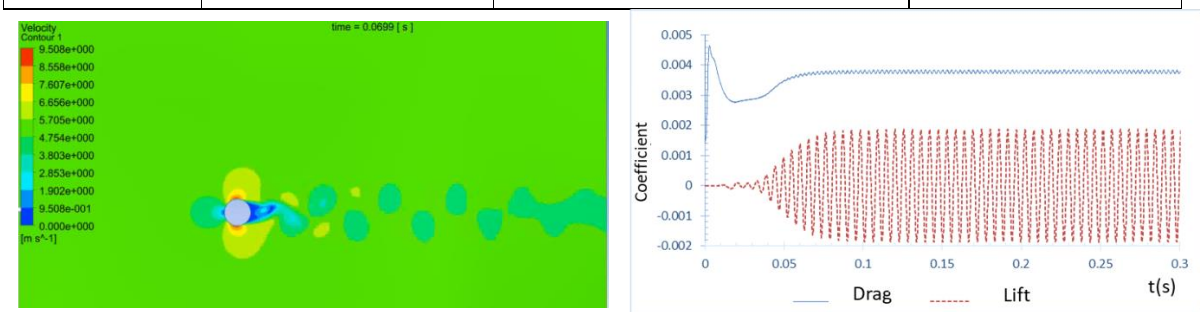

a) Appearance of vortex shedding behind the typical cross-section of thermowell

b) Lift coefficient and drag coefficient variations of thermowell

Fig. 6. 2D Fluent vortex shedding (case 1)

According to the previous result, the selected Case 1 was chosen for FSI analysis to find the location and value of stress concentration on the thermowell tube. Figure 7 shows the vortex shedding appears behind the thermowell in both scenarios of FSI analysis. The changes in the diameter from the root to the top of the thermowell resulted in the differences in size and time of vortex shedding's appearance. In the case of one-way FSI, the flow pressure will be mapped on the thermowell surface to calculate the deformation and stress concentration. However, no reversed feedback process on the flow field could occur. In the case of two-way FSI, the deformation information will be feedback to the flow field to calculate the influence of deformation on the flow. Because of the intensive interaction between sodium flow and thermowell, the lift force and drag force are changed. Their change makes the thermowell oscillated around the equilibrium position. As a result, the thermowell was bent by these forces that similars to thermowell configuration [8].

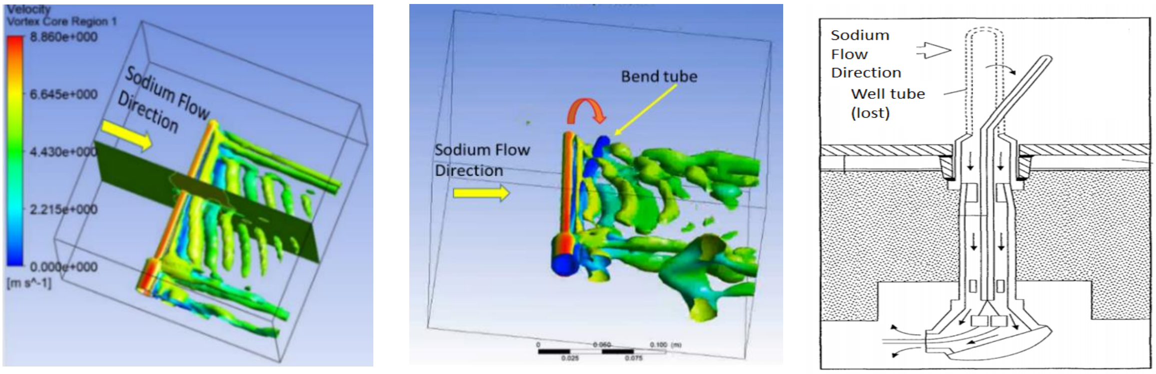

a) One-way FSI b) Two-way FSI c) Thermowell configuration [8]

Fig. 7. Appearance of vortex shedding behind the thermowell

Figure 8 shows that the location of stress concentration on the thermowell in FSI analysis is found in the place of the notch which is the same broken location of thermowell in the accident [8] for both cases one-way FSI and two-way FSI. However, the value of stress concentration is very different between the two types of FSI analysis. The maximum equivalent stress of 18.6 MPa in one-way FSI is much smaller than that in the case of two-way FSI. The results show a big difference between the structural response of static and dynamic load. The one-way FSI could not lead to fatigue damage because the endurance limit of structural steel is 86.2 MPa.

On the other hand, in two-way FSI, the absolute value of the maximum equivalent stress curve shows almost harmonic behavior (Figure 9). Although the time of simulation is short, which is enough time to observe the thermowell oscillating a few times. It is seen that only the first thermowell oscillating period is unstable, but the maximum equivalent stress of other periods is still greater than the endurance limit which could cause fatigue damage. The obtained result of two-way FSI gives a similar phenomenon that happened in the Monju accident.

The difference of results between one-way FSI and two-way FSI can be caused by pressure load. The static load in one-way FSI could not have resonance effects like dynamic load in two-way FSI in which the resonance could lead the system to oscillate with larger amplitude and maximum stress. In one-way FSI simulation, the fluid domain was not updated when the thermowell deformation happened. Differences in the pressure field lead to more conservative deflection values, whereas two-way FSI simulations updated the fluid domain related to the thermowell deformation at each time step. However, this approach needs a higher computational cost.

Although the calculation value of maximum equivalent stress two-way FSI is higher than the endurance limit, this study does not provide a complete picture of the assessments due to limitations in the computational resources. Therefore, further analysis for observing the behavior of stress concentration on thermowell need to be done in the future.

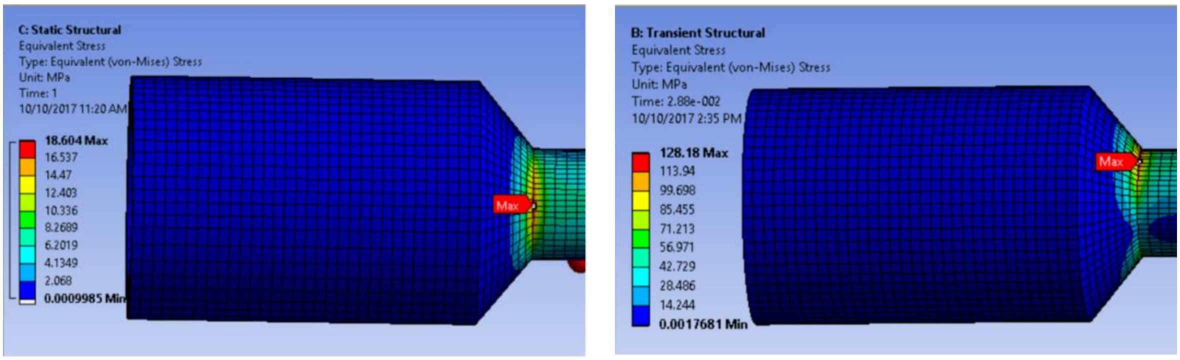

a) One-way FSI b) Two-way FSI

Fig. 8. Stress concentration on thermowell

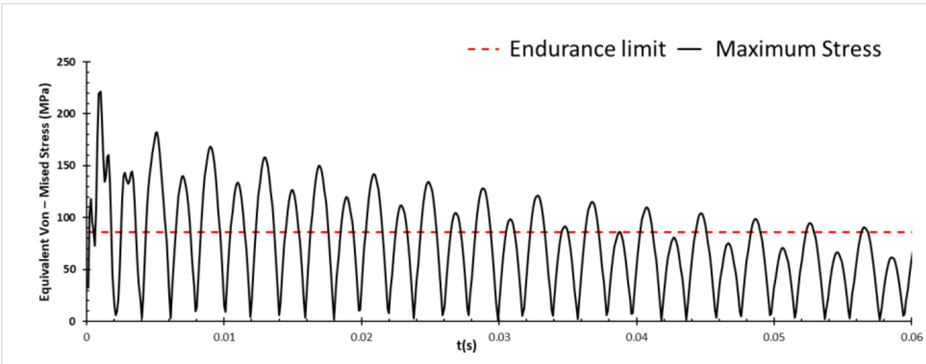

Fig. 9. Maximum equivalent stress (two-way FSI)

IV. CONCLUSIONS

In this study, two approaches of one-way FSI and two-way FSI using for analysis were performed to investigate the VIV phenomenon and the stress concentration location and the stress amplitude acting on Monju's thermowell. The flow condition with maximum stress was chosen for FSI analysis to find the most severe case leading to thermowell fatigue damage. The obtained result shows that fatigue damage initiated at an early stage of the 100% flow operation.

- In both approaches, the vortex shedding appears behind the thermowell. The changes in the diameter from the root to the top of the thermowell resulted in the differences in size and time of vortex shedding's appearance.

- The one-way FSI approach predicts well the stress concentration location. However, the value of the maximum equivalent stress at that location is not predicted with enough accuracy. In opposite, for the two-way FSI, it could predict both the stress concentration location and the value of the maximum equivalent stress at that location. Therefore, a two-way FSI approach for the evaluation of the stress on the thermowell of the Monju reactor is suitable.

- Fatigue damage could occur in the condition of the maximum value of stress getting higher than the endurance limit. This condition is reached in our analysis using two-way FSI. However, it is needed a longer time of simulation to observe the change in the stress amplitude for the overall fatigue damage process.

ACKNOWLEDGMENTS

The authors of this paper wish to express their appreciation for the financial support from VIETNAM ATOMIC ENERGY INSTITUTE (VINATOM) through the R&D Project: "Fluid – Structure Interaction (FSI) of sodium leakage incident at prototype fast breeder reactor Monju by ANSYS".

REFERENCES

[1]. H. Mikami, A. Shono and H. Hiroi, “Sodium Leak at Monju (I) - Cause and Consequences”, Tech. Committee Meeting on Evaluation of Radioactive Materials Release and Sodium Fires in Fast Reactors, Oaria, Ibaraki, Japan, International Atomic Energy Agency, Vienna, Austria, 1996.

[2]. Masaya Kondo, Yoshinari Anoda, “Water Flow Simulation Test on Flow – Induced Oscillation of Thermowell in Prototype Fast Breeder Reactor MONJU”, JSME International Journal, Serires B, Vol.4, No.4, 2001.

[3]. Hideki Aoi, Yue Zhao, Tamotsu Hayase, “Improvement of the Damaged Thermowell of the Monju Fast-Breeder Reactor Based on Vibration Analysis”, The Society for Modeling and Simulation International, SIMULATION, Vol. 78, Issue 8 , p. 504-511, 2002.

[4]. Sebastian Kornet, Daniel Sławiński, Paweł Ziółkowski, Janusz Badur, “Analysis of unsteady flow forces on the thermowell of steam temperature sensor”, Transactions of the Institute of Fluid-Flow Machinery, No. 129, p. 25–49, 2015.

[5]. AISI Type 304 Stainless Steel, [online] Available at:

http://www.matweb.com/search/datasheet.aspx?matguid=bd20a4281ae3430d97cfbebf6904ec50&ckck=1.

[6]. Masaki Morishita, Yusaku Wada, “Fatigue analysis of thermowell due to flow – induced vibration”, Flow – Induced Vibration and Transient Thermal – Hydraulics, ASME International, p. 120, 1998.

[7]. J.K.Fink, L.Leibowitz, “Thermodynamic and Transport Properties of Sodium Liquid and Vapor”, Argonne National Laboratory, pp. 86-95 and p. 207, 1995.

[8]. A.Miyakawa, H.Maeda, Y.Kami, K.Ito, “Sodium Leakage Experience at the Prototype FBR Monju”, Unusual Occurrences during LMFR Operation, IAEA-TECDOC-1180, Vienna (Austria), p. 43 -56, 1998.

[9] Anton Gustafsson, “Analysis of Vortex-Induced Vibrations of Rises”, Master’s thesis in Applied Mechanics, Chalmers University Of Technology, Sweden 2012.

[10]. Brauschke D., Wiklund D., Kitzman A., Zulic D., “Thermowell calculations”, Emerson Process Management, White Paper 00840–0200–2654, Rev AC, p. 11, March 2014.

[11]. ANSYS Tutorials & Training Materials, “Fluid Structure Interaction FSI with ANSYS Fluent 17.0” and “ANSYS Mechanical Linear and Nonlinear Dynamic”, ANSYS Inc, 2016.

[12]. Glück, M., Breuer, M., Durst, F., Halfmann, A., Rank, E., “Computation of fluid–structure interaction on lightweight structures”, Journal of Wind Engineering and Industrial Aerodynamics 89, p. 1351–1368, 2001.